Rev. LatinAm. Metal. Mat.

Artículo Regular

www.rlmm.org

CHARACTERIZATION OF LOW-ALLOY STEELS BY MEANS OF DIFFERENT TECHNIQUES

Juan Carlos González[*] *and Ney Luiggi*[**]

Grupo Física de Metales. Departamento de Física. Escuela de Ciencias. Núcleo de Sucre. Universidad de Oriente. Cumaná, Venezuela.

**e-mail: jcgonzal07@gmail.com ; **e–mail: nluiggi51@gmail.com*

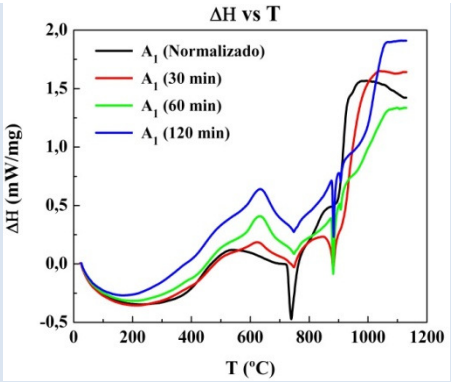

ABSTRACT

Two low carbon steels with different concentrations of carbon, one with manganese as its principal alloy component, were studied using electrical resistivity, Differential Scanning Calorimetry (DSC), Optical Microscopy (OM) and Scanning Electron Microscopy (SEM) as experimental techniques to study the kinetic of phase changes occurring during a non-isothermal heating in normalized and austenized microstructures. The measurements of electrical resistivity were used to test the austenization process at 1100ºC, showing how sensitive this method is to the concentration of solute in the samples. The resistivity being slightly larger at the onset, possibly due to the precipitation of carbides, and becoming slightly erratic and diminished as the aging time increases. For DSC, measurements were taken at different heating rates, which demonstrated different exothermic and endothermic transformations, indicative of the initial microstructure of the samples. Austenization introduces a new endothermic reaction, not present in the normalized samples, very localized and basically associated with the dissolution of martensite. Optical and scanning electron microscopy allowed us to visualize the granular state of the samples and follow the sequence of evolution of phases present in these steels, the normalized state showing a matrix rich in ferrite and pearlite, and all the treated samples showing a matrix rich in martensite, product of rapid tempering. The activation energies, for the endothermic reactions corresponding to the allotropic transformations $\alpha \rightarrow \alpha + \gamma$ and $\alpha + \gamma \rightarrow \gamma$., calculated by isoconversión methods are in the neighborhood of 22.2 y 26.7 Kcal/mol for the first and second endothermic processes, respectively.

Keywords: *Low-Alloy Steels, DSC, SEM, Activation Energy.*

CARACTERIZACIÓN DE ACEROS DE BAJA ALEACIÓN POR MEDIO DE DIFERENTES TÉCNICAS

RESUMEN

Dos aceros-bajos en carbono- con diferentes concentraciones de carbono, uno de ellos con manganeso como aleante principal, fueron estudiados usando resistividad eléctrica, calorimetría diferencial de barrido (DSC), microscopía óptica (MO) y microscopía electrónica de barrido (MEB) como técnicas de medición experimental para caracterizar la cinética de los cambios de fase que se producen durante un calentamiento no isotérmico en microestructuras normalizadas y austenizadas. Las mediciones de resistividad eléctrica se usaron para chequear la austenización a 1100 ºC, reflejando la sensibilidad de este método a la variación de la concentración de soluto en las muestras. La resistividad es ligeramente superior en el inicio, posiblemente debido a la precipitación de carburos, fluctúa y disminuye a medida que aumenta el tiempo de envejecimiento. Para DSC, las medidas fueron realizadas a diferentes velocidades de calentamiento, ocurriendo diferentes transformaciones exotérmicas y endotérmicas, indicativas de la microestructura inicial de las muestras. El proceso de austenización introduce una nueva reacción endotérmica, no presentes en las muestras normalizadas, muy localizados y, básicamente relacionadas con la disolución de la martensita. La microscopía óptica y electrónica de barrido nos permitió visualizar el estado granular de las muestras y seguir la secuencia de la evolución de las fases presentes en estos aceros. La microestructura normalizada muestra una matriz rica en ferrita y perlita, y todas las muestras tratadas muestran una matriz rica en martensita, producto de temple rápido. Las energías de activación para las reacciones endotérmicas que corresponde a las transformaciones alotrópicas $\alpha \rightarrow \alpha + \gamma$ y $\alpha + \gamma \rightarrow \gamma$ calculadas por isoconversión se encuentran en torno a 22,2 y 26,7 Kcal / mol para los procesos endotérmicos primero y segundo, respectivamente.

Palabras Claves: *Acero de baja aleación, DSC, MEB, Energía de Activación.*

1. INTRODUCTION

The principal product of the iron and steel industry is steel, 90% of the production being carbon steel, and 10% alloyed steel. Therefore, the metallic material most important for industry is carbon steel. Carbon steel is an alloy of complex chemical composition. In addition to iron, whose content can range between 97.0 and 99.5%, there are many elements whose presence is due to the production process (manganese and silicon), to the difficulty of completely excluding them from the metal (sulfur, phosphorus, oxygen, nitrogen, and hydrogen), or to chance circumstances (chromium, nickel, copper, and others) [1]. Increasing the carbon content in steel yields higher resistance to traction and results in reduced tenacity and ductility. These steels have a higher fragility index at ambient temperature. A vast number of vehicles, machines, installations, and countless parts are manufactured with these steels [2].

Studies on low carbon steel abound in the literature. They mainly focus on the effect that alloying elements have on the microstructure and precipitation of second phase particles, mechanical properties, and thermal aging treatments, but do not consider the kinetics of phases on the improvement of their properties [3, 4, 5, 6]. The objective of this work is to study the influence of the thermal treatments of austenization and quenching on the kinetics of non-isothermal phase transformations of low carbon steels, using the experimental techniques of electrical resistivity (ρ), differential scanning calorimetry (DSC), optical microscopy (OM), and scanning electron microscopy (SEM). We also determined the activation energy which is a typical parameter associated with the process of phase transformations [7].

2. EXPERIMENTAL PART

The low carbon steel alloys were supplied by CVG Siderurgica del Orinoco, C.A. Table 1 shows their nominal chemical composition.

The low alloy steel samples of table 1 will be studied under the normalized or as-received condition and under the austenized and quenched condition.

For samples used in the measurements of DSC, OM and SEM, the austenization treatment was performed at 1100 ° C in an electric furnace in an atmosphere of argon for 120 minutes, while for the electrical resistivity measurements, in order to verify the austenization degree, the samples were kept at the same temperature at intervals of 15, 30, 45, 60, 75, 90, 105 and 120 minutes.Once the heating was finished, the samples were immediately quenched in water at 25ºC. The electrical resistivity was measured using the Van der Pauw method [8] in a 25ºC isothermal environment. For each sample, eight (8) measurements were taken, always applying a 1A current between the contacts of the material, and reading the voltage between the contacts. For DSC a NETZSCH STA 449C differential scanning calorimeter was used on samples of approximately 30 mg mass each, both in normalized state and aged at 1100ºC for 120 minutes. The heating rates ϕ for DSC were 5, 10, 20 and 40ºC/min. The microstructure was examined with an Olympus CK40M-F100 brightfield optical microscope using reflected light. Subsequently, the samples were polished using disks with special cloths and 6 µm and 1 µm diamond paste. Finally, the samples were immersed in a 5% Nital solution for between 30 seconds and one minute. A HITACHI S-800 scanning electron microscope with an acceleration voltage of up to 30 kV was used for electron microscopy.

Table 1. Chemical composition of steels in %wt.

	Alloying Elements					
Low – Alloy Steels	**%C**	**%Mn**	**%Si**	**%Ni**	**%Cu**	**%Al**
A_0	0.1			< 1 %		
A_1	0.21	1.03	0.2	0.06	0.17	0.03

3. RESULTS AND DISCUSSION

Figure 1 shows the electrical resistivity of the steels studied, measured at ambient temperature, in function of the austenization time at 1100ºC. The electrical resistivity value corresponds to an average of eight current-Voltage measurements made with very precise instruments, so that the error or average deviation never exceeding 2% of reading. A slight increase in resistivity values is observed at the onset, possibly due to the precipitation of fine carbides taking advantage of the concentration of vacancies during tempering. Subsequently, as the annealing

time increases, there is a gradual reduction in resistivity due to the dissolution of carbides in the austenite, a process which increases the quantity of carbon in this phase, a greater quantity of martensite being thus retained after tempering. We observe that the greatest resistivity corresponds to carbon steel A_1 containing 0.21%wt of C, the sensitivity of this property depending upon the quantity of solute in the alloy. The variation in resistivity relative to the initial value, where there is no martensite, corresponds principally to the contribution of this phase to the resistivity.

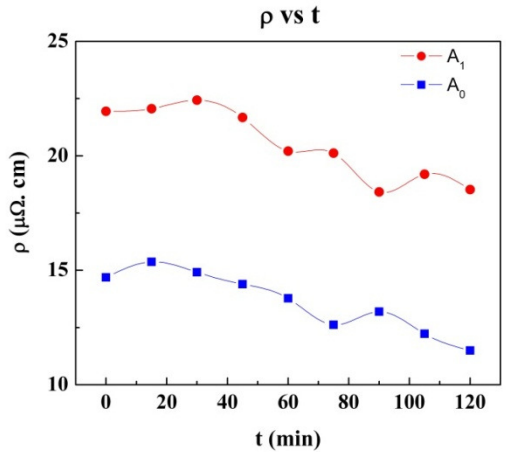

Figure 1. Electrical resistivity of A_0 and A_1 steels, as a function of the austenization time at 1100ºC, measured at ambient temperature.

Figure 2 shows the variation of heat flux as a function of temperature for the steels studied, heated at rates of 5, 10, 20, and 40ºC/min. For the A_1 steel in its normalized state (figure 2a), a series of valleys and peaks indicative of the different processes occurring is observed. In this heat flux diagram, we identify a broad valley whose minimum value is about of 250ºC, followed by sharp and very distinct endothermic transformation at 745ºC, and by a new exothermic transformation within the austenitic region. The two exothermic reactions seem to occur by diffusion due to their displacement with the variation in heating rate, unlike the second endothermic reaction, whose displacement with Φ is very small. The first endothermic reaction shows a displacement different from that obtained when the processes occur by diffusion. The effect of the austenization is shown in the heat flux diagram in figure 2.b, where the A_1 sample was annealed at 1100ºC for 120 minutes. The effect of this treatment is to carry the carbides and atomic conglomerates present in the normalized steel to the austenitic solution. As the treatment continues, more carbide is dissolved, in such a way that rapid quenching will trap more carbides in the austenitic matrix, and as such, the fraction of martensite formed in these cases must be greater. The heat flux diagram for this case shows the same behavior as in the previous case, plus a sharp endothermic transformation at 870ºC. It is worth pointing out that the temperatures of the peaks in the endothermic processes move slightly to the right as the heat rate decreases.

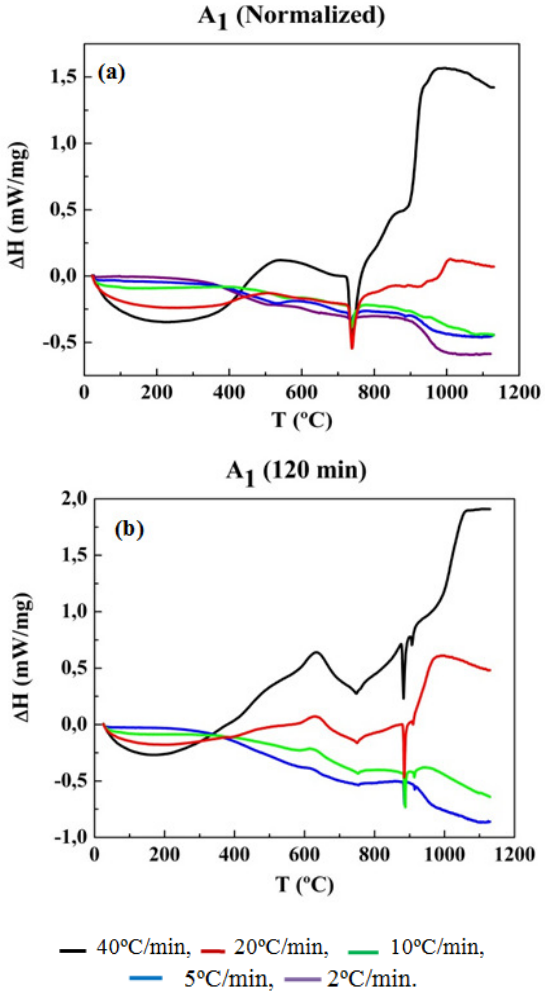

Figure 2. Heat flux vs T for A1 steel for different heating rates. (a) Normalized. (b) Austenized at 1100ºC.

In Figure 3.a, for the A_0 steel in normalized state, was identified a broad valley whose minimum value is placed about of 200ºC, followed by an exothermic transformation whose maximum is at 550ºC. Subsequently, two small, closely spaced endothermic processes appear, that tend to grow

apart from each other considerably as the sample ages, the peak temperature moving towards the lower temperatures as the heating rate is reduced, to end up with a new exothermic transformation, this time within the austenitic region. In all cases, the first localized peak is related to the allotropic transformation process of $\alpha \rightarrow \alpha + \gamma$, and the second peak, to the $\alpha + \gamma \rightarrow \gamma$ transformation of the phase diagram. The first endothermic transformation, or broad valley, corresponds to the dissolution of carbides in normalized samples and of martensite in the aged samples, while the first exothermic transformation corresponds to the formation or precipitation of carbides. The last exothermic transformation is related to the austenization process.

Figures 4 and 5 show the evolution of the transformed fraction in function of temperature for the steels studied, considering different values of Φ, calculated for the regions where the first isolated endothermic transformation occurs. Similar behavior is obtained for the second endothermic transformation. The general behavior is sigmoidal, small movements and overlapping of the curves at the point of transformation being observed as the heating rate Φ increases, which could lead us to think that the mechanism responsible for this change is not essentially diffusive. The activation energy is then determined from the transformed fraction After the transformed fraction, we proceeded to determine the activation energy according to the iso-conversional scheme [9] for a fixed value of N = 2, and according to Kissinger's equation [10]. See Reference [7] for details of this calculation.

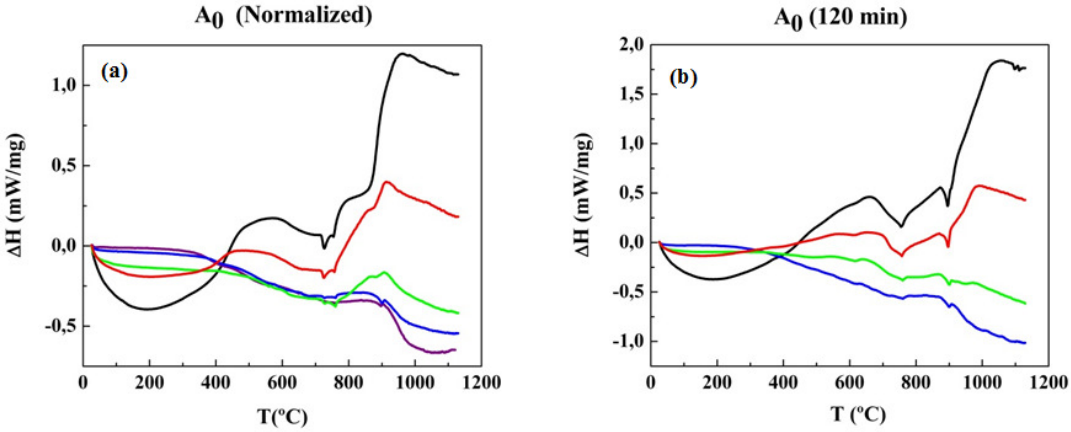

Figure 3. Heat flux vs T for A_0 steel for different heating rates. Same legend as in Figure 2.

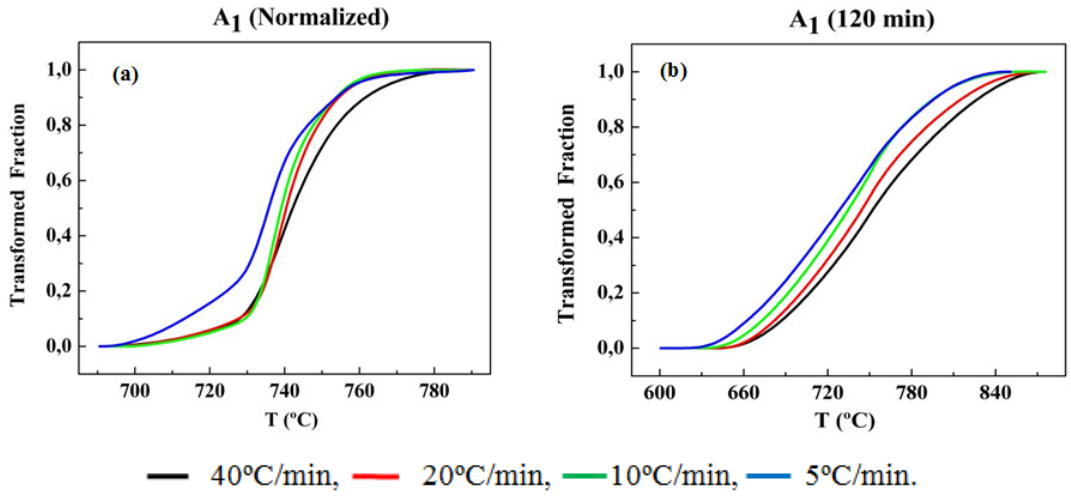

Figure 4. Transformed fraction as a function of temperature for A_1 steel for the first endothermic process, for different heating rates (a) Normalized. (b) Aged for 120 minutes.

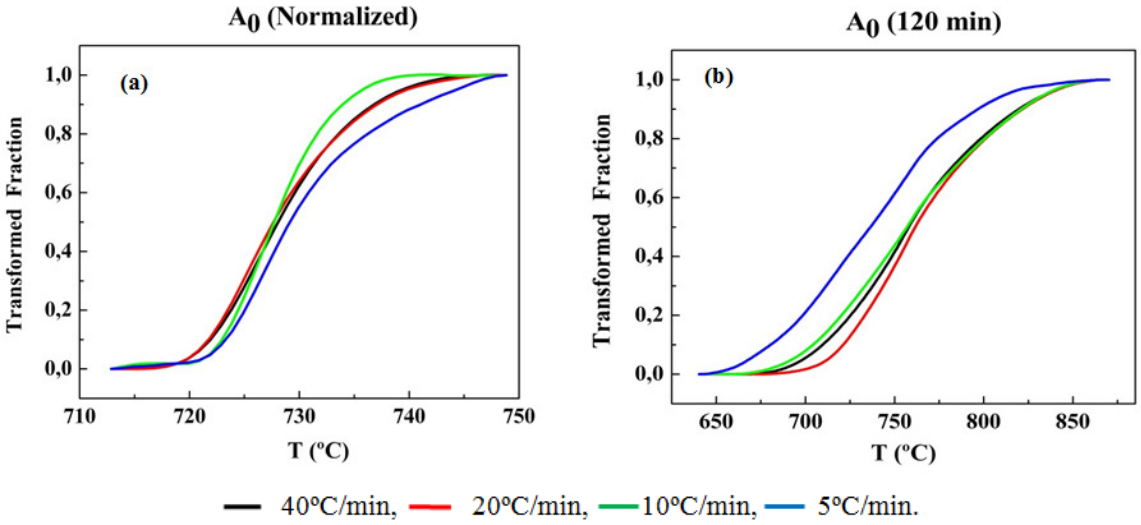

Figure 5. Transformed fraction as a function of temperature for A_0 steel for the first endothermic process, for different heating rates. (a) Normalized. (b) Aged for 120 minutes.

In Figures 6 and 7, the activation energies are graphed in function of the transformed fraction for the A_1 and A_0 steels in the first two punctual endothermic processes corresponding to the two allotropic transformations $\alpha \rightarrow \alpha + \gamma$ and $\alpha + \gamma \rightarrow \gamma$. In each case, the iso-conversional calculation predicts an increase of Q with Y, indicating that multiple mechanisms occur in that reaction [7], whereas the value deduced from Kissinger's equation remains constant. Also note the tendency in the first peak of the normalized steel to present a constant value of Q, even in the iso-conversional calculation. Table 2 summarizes the values of activation energy for both peaks using Kissinger's equation and the iso-conversional average, respectively. In general, both methods produce consistent results, demonstrating the need for greater activation energy for the second process.

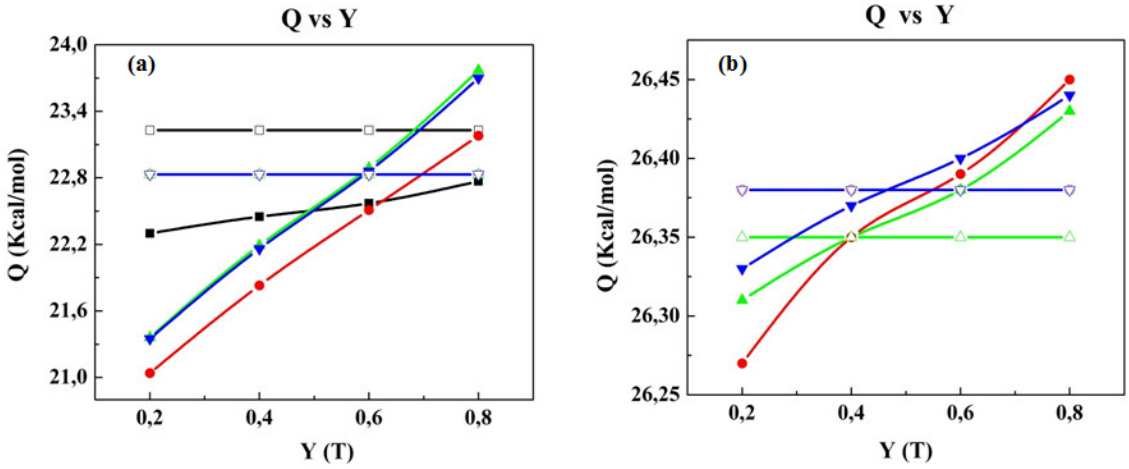

Figure 6. Activation energy (Q) vs. Transformed fraction (Y) obtained using both Kissinger's equation and the non-isothermal iso-conversional scheme for N = 2, for the two endothermic processes present in the A_1 steel for different times of thermal treatment. a) First endothermic peak. b) Second endothermic peak. Kissinger: □ Normalized ○ 30 min, △ 60 min, ▽ 120 min. For N = 2: ■ Normalized, ● 30 min, ▲ 60 min, ▼ 120 min.

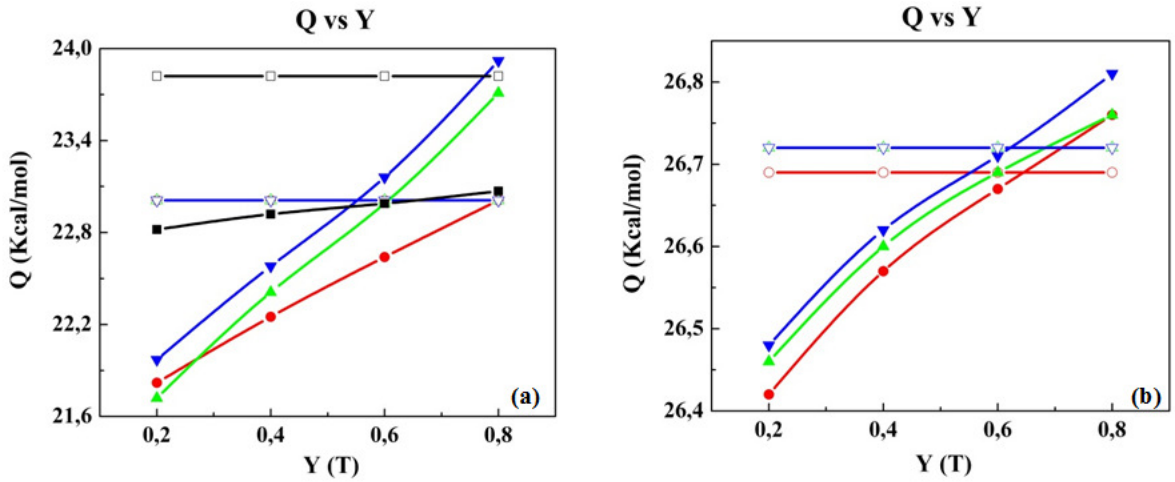

Figure 7. Activation energy (Q) vs. Transformed fraction (Y) obtained using both Kissinger's equation and the non-isothermal iso-conversional scheme for N=2, for the two endothermic processes present in the A_0 steel for different times of thermal treatment. a) First endothermic peak. b) Second endothermic peak. Kissinger: □ Normalized ○ 30 min, △ 60 min, ▽ 120 min. For N = 2: ■ Normalized, ● 30 min, ▲ 60 min, ▼ 120 min.

Table 2. Activation energies of the two allotropic transformations for the two steels studied, at different aging times, applying Kissinger's equation and the iso-conversional method for N = 2.

Aging Time	A_0 *Kissinger* *Q (Kcal/mol)*	A_1 *Kissinger* *Q (Kcal/mol)*	A_0 *Iso-conversion N=2* *Q (Kcal/mol)*	A_1 *Iso-conversion N=2* *Q (Kcal/mol)*
Normalized	22.91	23.23	22.23	22.52
	23.82		22.95	
30 min	23.01	22.83	22.43	22.14
	26.69	26.38	26.61	26.37
60 min	23.01	22.83	22.71	22.55
	26.72	26.35	26.63	26.37
120 min	23.01	22.83	22.91	22.52
	26.72	26.38	26.66	26.39

The microstructure of the different steels, normalized and annealed at 1100ºC for 120 minutes, are shown in the photomicrographs 8.a and 8.b. In normalized state, a structure is observed composed of polygonal ferrite, acicular ferrite, and pearlite nodules: that is to say, a ferrite-pearlite structure. As the carbon content increases in the steels studied, the proportion of pearlite increases slightly. Photomicrographs 8.c and 8.d show that as the steels are aged for 120 minutes, followed by quenching in cold water; the formation of martensite is observed (sub-grains that acquire an acicular morphology) on an austenite matrix. It should be pointed out that, in these samples, some zones are observed where the martensite has not completely formed.

Micrographs 9.a, 9.b, 9.e, and 9.f, obtained using scanning electron microscopy, correspond to the normalized state of A_1 y A_0 steels, taken at 1000X and 4000X. A good delineation of the grain boundaries is noticeable, as well as the presence of a ferrite-pearlite structure, where polygonal and acicular ferrite grains can be observed, and in detail the structure of the pearlitic constituent forming colonies oriented in the direction of the rolling. The pearlite is classified, according to the aggregation of the cementite, as sorbitic, lamellar, and granular pearlite, the latter being the most abundant. The acicular ferrite, observed with the scanning electron microscope, differs from polygonal ferrite in that the former, as a result of shearing, looks more like a

laminate with two parallel opposing borders, while the latter looks like a polyhedron with curved borders. Some precipitates in the ferrite grains are also observed. In micrographs 9.c, 9.d, 9.g, and 9.h for the A_1 and A_0 steels aged for 120 minutes at 1100ºC, the formation of the martensite structure with an acicular morphology can be observed on the austenitic grain, and some precipitates remain trapped in the matrix. It is worth noting that the A_1 steel has a more profuse pearlite formation in its normalized state than the A_0 steel, principally due to its greater carbon content. In the A_1 steel aged for 120 minutes, a greater formation of martensite is observed than in the A_0 steel.

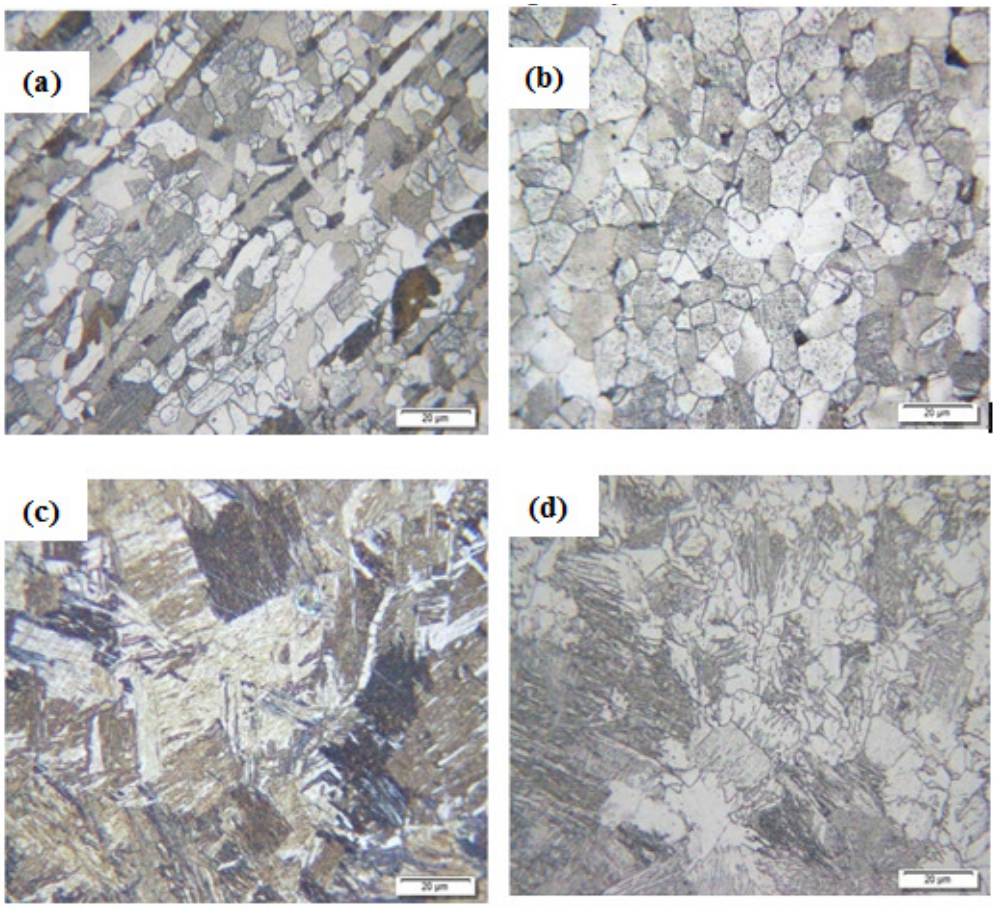

Figure 8. Photomicrographs at 500X. (a) and (b) Normalized A_1 y A_0 steels. (c) and (d) A_1 y A_0 steels aged for 120 minutes and quenched at 25ºC.

4. CONCLUSIONS

The effect of annealing at different times of austenization, followed by tempering, was to diminish the value of electrical resistivity compared to the value obtained in normalized samples; this variation can be explained as being due to the formation of the martensitic phase. The electrical resistivity also shows itself to be sensitive to the process of phase transformation predicting the multi-phase behavior, due to the presence of valleys and peaks that we associate with the precipitation and dissolution of different carbides. As the value of the %wt of C present in the steels increases, so does the value of electrical resistivity. The calorimetric measurements show the sensitivity of the heat flow to the thermal treatment, showing a different behavior in the austenized samples compared to that obtained in the normalized state. At least five generic transformations are reported in the austenized and quenched samples, associated with the initial restructuring of the alloy components and the presence of martensite tempered below the eutectic point, which is dissolved in a first exothermic transformation, followed almost

immediately by two nearly distinct endothermic peaks whose temperatures move slightly as the heating rate diminishes. The austenized and quenched samples introduce an endothermic transformation not present in the normalized ones, attributed to the dissolution of martensite formed during tempering. Optical and scanning electronic microscopy allowed us to follow the sequence of evolution of the different phases present in these steels, revealing a ferro-pearlitic structure in their normalized state and the formation of martensite when thermally treated, after swift quenching in cold water. Also observed were some precipitates that possibly retard the total formation of the martensitic phase. The average activation energy associated with the discrete processes, calculated iso-conversionally, range between 22.14 kcal/mol and 22.95 kcal/mol for the first endothermic process, and between 26.37 kcal/mol and 26.66 kcal/mol for the second. Kissinger's equation gives values ranging between 22.83 kcal/mol and 23.82 kcal/mol and between 26.35 kcal/mol and 26.72 kcal/mol for the first and second endothermic processes, respectively, showing a good concordance.

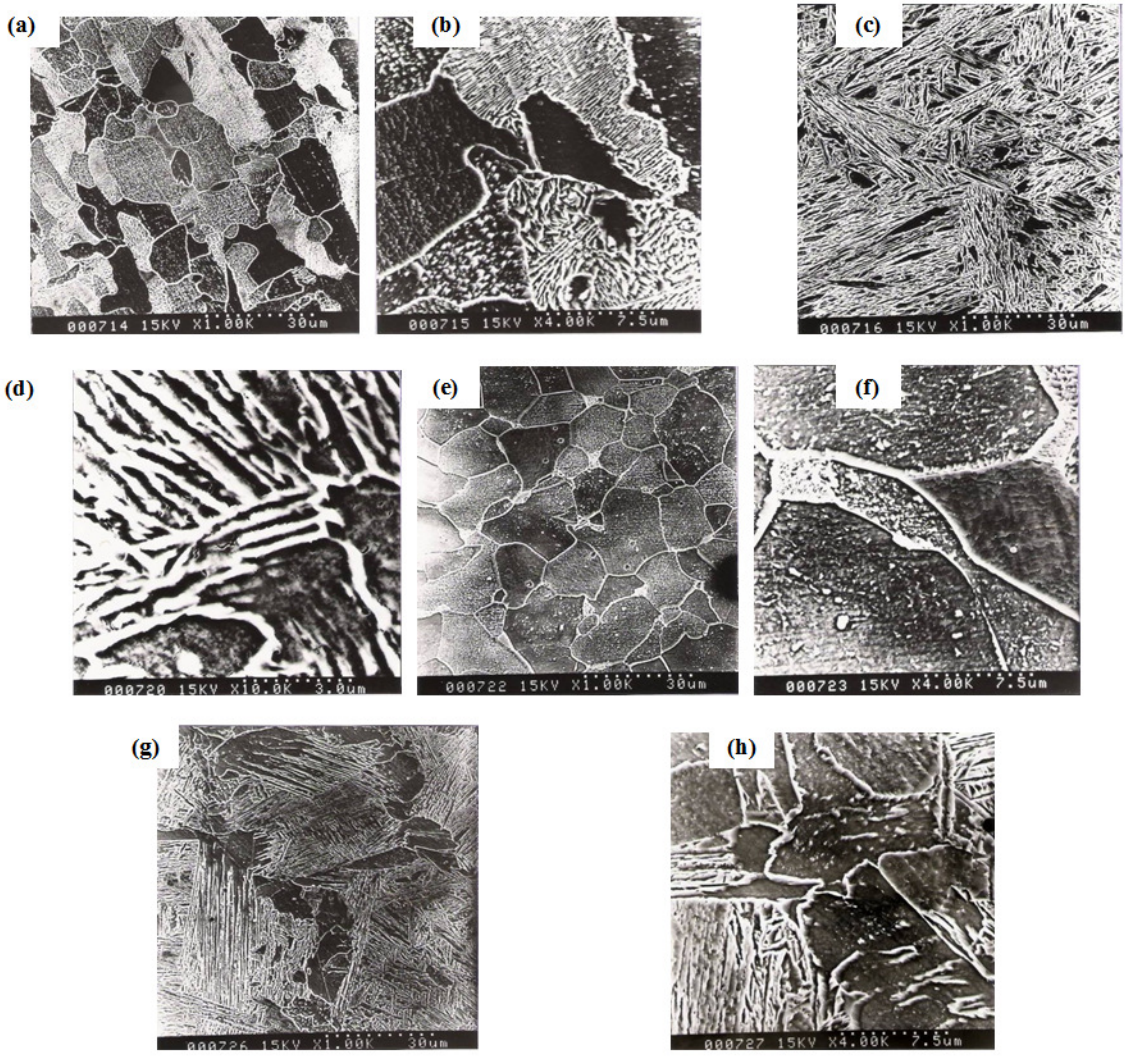

Figure 9. Micrographs of A_1 steels: (a) and (b) normalized, at 1000X and 4000X, (c) and (d) aged for 120 minutes at 1000X and 10000X. A_0 steels: (e) and (f) normalized at 1000X and 4000X, (g) and (h) aged for 120 minutes, at 1000X and 4000X.

5. ACKNOWLEDGEMENTS

The authors want to agree the financial support of the Consejo de Investigación de la Universidad de Oriente.

6. REFERENCIAS

[1]. Sage AM. J. Mine. Met. Mater. Soc. 1990; p. 51–60.

[2]. Korchinsky M. Proceedings from materials solutions Conference. 2002; p. 2.

[3]. Bejar L; Medina A and Martínez R. Rev. Latin. Am. Met. Mat. 2003; 23: 59–62.

[4]. San Martín D, Caballero FG, Capdevilla C. Rev. Metal. 2006; 42: 128–137.

[5]. Illescas S, Fernández J, Guilemany JM. Revista de Metalurgia. 2008; 44 (1): 39–51.

[6]. González L. Estudio de la tenacidad al impacto que presentan algunos aceros de medio carbono microaleados. Tesis Doctoral en Ciencias de los Materiales. Universidad Central de Venezuela (Venezuela) 2004.

[7]. González JC. Caracterización de Aceros de Baja Aleación y Microaleados al Mo por diferentes técnicas, Tesis de Maestría en Física. Universidad de Oriente (Venezuela) 2009.

[8]. David T; Moldchadsky I; Somechi A. and Rosenbaum R *Novel Analog Switching Circuit for Van der Pauw Measurements*. Technical Paper, available on the arxiv e-print

[9]. Luiggi N, Betancourt M. J. Therm. Anal. Calorim. 2003; 74: 883–894.

[10]. Kissinger HJ. Res. Nat. Bur. Stan. 1956; 57: 217–222.